JCI The Journal of Clinical Investigation

Inhibition of estrogen signaling in myeloid cells increases tumor immunity in melanoma

Binita Chakraborty, … , Ching-Yi Chang, Donald P. McDonnell

J Clin Invest. 2021. https://doi.org/10.1172/JCI151347.

Research In-Press Preview Oncology

Graphical abstract

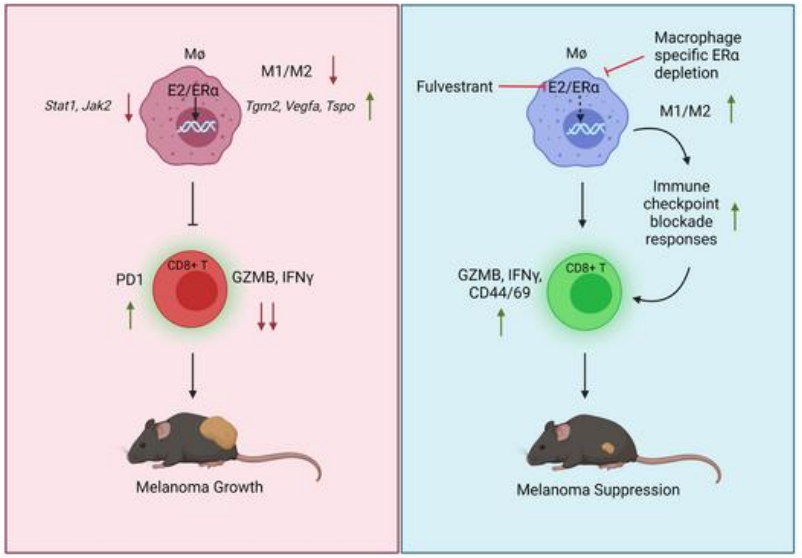

Inhibition of estrogen signaling in myeloid cells increases tumor immunity in melanoma

Binita Chakraborty[1], Jovita Byemerwa[1], Jonathan Shepherd[2], Corinne Haines[1], Robert Baldi[1], Weida Gong[2], Wen Liu[1], Debarati Mukherjee[1], Sandeep Artham[1], Felicia Lim[1], Yeeun Bae[1], Olivia Brueckner[1], Kendall Tavares[1], Suzanne Wardell[1], Brent Hanks[3], Charles Perou[2], Ching-Yi Chang[1] and Donald P. McDonnell[1]*.

[1]Department of Pharmacology and Cancer Biology, Duke University School of Medicine, Durham, NC, USA

[2]Lineberger Comprehensive Cancer Center, University of North Carolina at Chapel Hill, Chapel Hill, NC, USA

[3] Department of Medicine, Duke University School of Medicine, Durham, NC, USA

*Corresponding author: donald.mcdonnell@duke.edu

Telephone number: 919-684-6035

Mailing address: Box 3813, Durham, NC, USA

Abstract

Immune checkpoint inhibitors (ICB) have significantly prolonged patient survival across multiple tumor types, particularly in melanoma. Interestingly, gender specific differences in response to ICB have been observed with males getting more benefit than females, although the mechanism(s) underlying this difference are unknown. Mining published transcriptomic datasets, we determined that response to ICBs is influenced by the functionality of intratumoral macrophages. This puts into context our observation that estrogens (E2) working through the estrogen receptor (ERα) stimulate melanoma growth in murine models by skewing macrophage polarization towards an immune-suppressive state that promotes $CD8^+$ T cell dysfunction/exhaustion and ICB resistance. This activity was not evident in mice harboring a macrophage specific depletion of ERα confirming a direct role for estrogen signaling within myeloid cells in establishing an immunosuppressed state. Inhibition of ERα using fulvestrant, a selective estrogen receptor downregulator (SERD) decreases tumor growth, stimulates adaptive immunity and increases the antitumor efficacy of ICBs. Further, a gene signature that reads on ER activity in macrophages predicted survival in ICB treated melanoma patients. These results highlight the importance of E2/ER as a regulator of intratumoral macrophage polarization; an activity that can be therapeutically targeted to reverse immune suppression and increase ICB efficacy.

Introduction

Metastatic melanoma is one of the most aggressive, morbid cancers with a median survival of 6-9 months (1). Whereas the development of MAPK-pathway inhibitors and antibodies directed against immune checkpoints have significantly improved outcome in this disease, *de novo* and acquired resistance to these therapies remains a major impediment to achieving durable clinical responses in most patients (2-5). Further, although complete responses to combination immune checkpoint blockade (ICB) therapies (α-CTLA4+α-PD1) occurs in ~20% of patients (6), the general toxicity and immune related adverse events seen in the majority of individuals receiving existing combination therapies significantly limits their clinical use (7). Thus, strategies that increase the efficacy and/or reduce the toxicities associated with ICB would likely expand the clinical utility of existing drugs and ultimately improve long-term outcomes in this disease.

The classification of melanoma as a hormone-sensitive neoplasm remains controversial and the importance of hormone associated risk factors, such as pregnancy, menopausal status, hormone therapies and the use of oral contraceptives, on the pathobiology of this disease remains unclear (8-12). While the potential effects of sex steroids on melanoma risk needs to be assessed in large clinical studies, there already exists compelling evidence that the incidence of secondary melanoma is significantly lower in anti-estrogen treated breast cancer patients than in the general population (13). Further, the results of a recently published meta-analysis revealed that the degree of benefit from ICB in melanoma, and in patients with non-small cell lung cancer, is lower in women than in men (14). Considering these observations, we hypothesize that there are sex hormone-dependent baseline differences in the immune system that contribute to gender specific differences in tumor immunity and ICB efficacy. Under normal physiological conditions and in some disease contexts it has been demonstrated that female sex steroids that target the estrogen receptor (ER) affect the differentiation and function of both the humoral and adaptive immune systems (15). However, the extent to which estrogen action/signaling in the tumor-immune

66 microenvironment impacts the growth of melanoma and if and how this signaling axis can be
67 exploited for therapeutic benefit has not been established.

68 Estrogens mediate their physiological actions in cells through the classical nuclear ERs (ERα and
69 ERβ) and through the non-classical G-protein coupled receptor GPER1 (also referred to as
70 GPR30). A recent study by *Natale et al* highlighted a tumor cell-intrinsic role for GPER1 in
71 regulating melanocyte differentiation, thereby preventing melanoma cell proliferation. Further, a
72 synergistic anti-tumor response was observed when GPER agonists were combined with immune
73 checkpoint inhibitors (16). While anecdotal evidence exists regarding the expression of nuclear
74 ERs in melanoma cancer cells, the extent to which these receptors play a role in tumor
75 progression remains to be determined (17). ERs have also been shown to be expressed in several
76 different cell types within the tumor microenvironment and likely play a role in determining tumor
77 response to ER modulators. Indeed, 17β-estradiol (E2) working through ERα expressed in
78 endothelial cells in the tumor microenvironment has been shown to induce tumor growth by
79 improving tumor angiogenesis and protecting tumor cells against hypoxia and necrosis (18).
80 Further, ER actions have been studied in different immune cell types in different diseases (19-
81 21), but the extent to which ER influences immune cell biology within the tumor microenvironment
82 has not been examined in detail. Recently, it has been demonstrated in ovarian cancer that E2
83 can create an immune suppressive tumor microenvironment (TME) by promoting the mobilization
84 of myeloid-derived suppressor cells (MDSC) from bone which function to suppress tumor
85 immunity and increase tumor growth (22). While this study demonstrates that ER function is
86 important for MDSC mobilization, the tumor microenvironment is infiltrated with multiple other
87 myeloid cell types such as dendritic cells (DCs), monocytes, and tumor associated macrophages
88 all of which impact tumor immunity (23). Notably, ERs have been shown to play a critical role in
89 development and functionality of these myeloid cell types (24, 25). However, the extent to which

ER function regulates myeloid cell-T cell crosstalk within the TME and how it affects ICB responses are not known.

In this study we have explored how E2 modulates immune cell function and repertoire within the melanoma TME and how this influences tumor growth in established murine models of this disease. Specifically, we have determined that a primary action of E2 is to facilitate the polarization of macrophages towards an immune-suppressive state in the tumor microenvironment, characterized by an enhanced ability to promote tumor growth and, in an indirect manner, suppress cytotoxic T cell responses. Further, we provide evidence that pharmacological inhibition of E2 signaling, using the Selective Estrogen Receptor Downregulator (SERD)/antagonist fulvestrant, reverses E2 enhanced melanoma tumor growth by stimulating the establishment and maintenance of a pro-immunogenic TME characterized by increased presence of activated CD8+ T cells. Importantly, in preclinical models of melanoma, fulvestrant treatment increases the efficacy of α-PD1 and α-CTLA4, providing the rationale for a clinical trial that will soon be initiated to evaluate the utility of combining contemporary SERDs with standard of care immunotherapies to maximize therapeutic response in melanoma patients.

Results

Decreased M1/M2 tumor associated macrophage (TAM) ratio compromises the benefit of ICB therapy in melanoma patients

Myeloid cell infiltration has been associated with poor outcomes in multiple cancer types (26-31). However, the extent to which tumor infiltrating myeloid cells influence response to immunotherapy in melanoma patients has not been explored. To address this issue, we evaluated potential correlations between the number and characteristics of tumor infiltrating myeloid cells and patient's response to ICB using published transcriptomic datasets from melanoma patients who had received standard of care immune checkpoint blockade (32-34). The predominant suppressive myeloid cells in the tumor microenvironment are myeloid derived suppressor cells (MDSC) and tumor associated macrophages (TAMs). To address whether MDSCs play a role in predicting patient response to ICB, we used a validated MDSC gene signature (35-39) to analyze transcriptomic data (32) from melanoma patients who have received α-PD1 (Nivolumab or Pembrolizumab) or α-CTLA4 (Ipilimumab) either alone or in combination. As shown in **Figure S1A-E**, MDSC signatures were not predictive of patient's response to ICB or survival. In contrast, signatures from CIBERSORT (39), that read on the polarization state of TAMs are useful in predicting ICB response in the same datasets (32). Notably, enrichment of the M1 gene signature in tumors was associated with better responses (increased number of complete responders (CRs) and partial responders (PRs)) when compared to patients with stable disease (SD) or progressive disease (PD) (**Figure 1A**). A similar trend in patient prognosis was also observed when patients were parsed as a function of high vs low intratumoral M1/M2 macrophage ratio (**Figure 1B**). Enrichment of the M2 signature alone did not correlate with patient prognosis (**Figure S2A**). Using the same dataset (32) we also addressed whether the macrophage gene signature is associated with overall survival in melanoma patients receiving immunotherapies. Similar to what was observed with patient prognosis (**Figures 1A and B)** an enrichment of either the M1 gene signature or the M1/M2 ratio gene signature, but not enrichment of the M2 signature, was

associated with better overall survival (**Figures 1C-D and S2B**). Interestingly, a positive association between the enrichment of an M1 gene signature, or the ratio of M1/M2 gene signature, with patient prognosis and survival was also noted when the patients were parsed for those who received α-PD1 monotherapy alone (**Figures S2C-H**), while those patients who received dual therapy showed a non-significant trend in this association (**Figures S2I-N**). Additionally, an increase in intratumoral M1/M2 ratio predicted better survival in melanoma patients in the TCGA SKCM dataset (**Figures S3A-C**). The prognostic utility of assessing the intratumoral M1/M2 macrophage ratio was confirmed in independent datasets derived from melanoma patients treated with immunotherapy (**Figure 1E**) (33, 34). It has been reported in several studies that gender influences patient response to immunotherapy in melanoma, with females receiving a lesser degree of benefit from ICB than males (14, 40). Motivated by these observations and previous studies demonstrating that female steroid hormone estrogens (E2) affect macrophage differentiation and polarization (19, 21), we hypothesized that estrogens may modulate the tumor microenvironment to promote immunotherapy resistance. It was of significance, therefore, that we observed that increased expression of *CYP19A1*, the enzyme that controls the rate-limiting step in estrogen biosynthesis, is correlated with increased TAM accumulation in ICB non-responsive melanoma patients (**Figures 1F-G**) (34). Importantly, stratification of patients based on tumor expression of *CYP19A1* mRNA revealed its elevated expression to be associated with the expression of the macrophage markers *CD68, CSF1, CSF1R* and the T cell exhaustion marker *PDCD1* (**Figure 1F**) in non-responders whereas no such associations were identified in responder patient populations (**Figure 1G**). These results suggest that E2 may be causally involved in the establishment of an immune suppressive tumor microenvironment through modulating TAM biology; a hypothesis that we proceeded to test experimentally.

E2 promotes melanoma tumor growth

The results of studies addressing whether ERs are expressed within melanoma cells/tumors are equivocal. While some studies have demonstrated low expression of ERα and ERβ in human melanoma tumors by immunohistochemical staining (IHC) (41, 42), the functionality of these receptors within tumor cells is unknown. Thus, we evaluated the expression of ERα in B16F10 and YuMM5.2 mouse melanoma cells following siRNA-mediated knockdown of *Esr1*. ERα+ MCF7 cells were used as a positive control for ERα expression. Weak ERα protein was detected in YuMM5.2 cells and this was depleted upon siRNA treatment (**Figure S4A-B**). By immunoblotting we were unable to detect ERα protein in B16F10 cells (a band migrating at approximately the same size as ERα was not depleted upon siRNA treatment despite a significant reduction of ERα mRNA (expressed at very low level)). Regardless, treatment of either cell with E2 did not lead to changes in the expression of classical ER target genes (*Pgr* and *Cxcl12*) (**Figure S4C**) nor did it support proliferation (**Figures S4D-E**). Collectively, these data validate the use of these cell models to study the cancer cell extrinsic actions of estrogens/ER modulators on the pathobiology of melanoma. To this end, B16F10, YuMM5.2, or BPD6 melanoma cells were injected subcutaneously into ovariectomized syngeneic mice supplemented with either placebo or E2 pellets (0.01mg/60 days continuous release). As expected, E2 administration results in an increase in uterine wet weights in the ovariectomized mice (**Figure S4F**). As shown in **Figures 2A-E**, E2 treatment significantly increases tumor growth in all three syngeneic models compared to placebo control mice. To further validate our observations in a more clinically relevant system, we used an autochthonous mouse model in which tumor growth was driven by concomitant conditional activation of B-Raf^{V600E} and homozygous deletion of *Pten* in melanocytes (*Braf*^{tm1Mmcm},*Pten*$^{f/f}$; mTyr-CreERT2, heretofore referred as iBP) (43). This mouse model faithfully resembles human melanomas harboring *BRAF* and *PTEN* mutations. Similar to the syngeneic models, administration of E2 in ovariectomized mice accelerated tumor growth in the iBP model

compared to the placebo counterparts (**Figures 2F-H**). The slower tumor growth kinetics that were imparted by ovariectomy disappeared when B16F10 cell derived tumors were grown in NOD.Cg-*Prkdc*^{scid} *Il2rg*^{tm1Wjl}/SzJ (NSG) mice (**Figure 2I**) suggesting that the actions of E2 on tumor growth were likely mediated by an immune cell(s).

E2 regulates the function of tumor-associated myeloid cells

To determine how E2 treatment affects the tumor immune microenvironment, we performed single cell RNA sequencing (scRNA seq) analysis of tumor infiltrating immune cells isolated from iBP tumors treated with either placebo or E2. Unsupervised clustering analysis using uniform manifold approximation and projection (UMAP) revealed global differences in tumor infiltrating immune cells when comparing placebo and E2 treatments and identified clusters of immune cells that have unique transcriptional profiles. Comparison of cell type signature(s) with the Immgen database and known cell type markers (**Supplementary File I**), resulted in the identification of 9 macrophage/myeloid clusters, 10 lymphoid clusters, 2 neutrophil clusters, 2 DC clusters and one B cell, NK cell and mast cell cluster (**Figures 3A and S5A**). Analysis of the scRNA seq dataset also revealed that the majority of *Esr1* transcripts are expressed in cells within the myeloid lineage, while the expression of *Esr2* and *Gper* were minimal to undetectable (**Figures S5B-D**). Differences in the immune cell repertoires from placebo and E2 treated tumors were also evident (**Figure S6A**). Notably, E2 treatment led to the expansion and significant changes in gene expression in the CD68^{+} monocytes/TAMs clusters (**Figure 3B and Figure S6B**) To determine the functionality of ER signaling in the monocyte/TAM cluster, we genetically depleted ERα in myeloid cells using a lysozyme-driven Cre-recombinase (*Esr1*$^{f/f}$; LysMCre) to establish its role(s) in tumor responses to E2. ERα depletion in the myeloid lineage was confirmed in bone marrow derived macrophages (BMDM) isolated from *Esr1*$^{f/f}$; LysMCre and littermate *Esr1*$^{f/f}$ controls (**Figure S6C**). Subsequently, 8-week old *Esr1*$^{f/f}$; LysMCre, and littermate control (*Esr1*$^{f/f}$ and LysMCre) mice, were used to evaluate syngeneic tumor growth in the B16F10 and Yumm5.2

models, in the presence or absence of E2. The growth of B16F10 and YuMM5.2 tumors increased in response to E2 in *Esr1*$^{f/f}$ and LysMCre mice but this was not evident in *Esr1*$^{f/f}$; LysMCre mice (**Figures 3C-D and S6D**). Analysis by flow cytometry of tumor infiltrating immune cells revealed a decrease in M1 (proinflammatory macrophages) in E2 treated *Esr1*$^{f/f}$ but not *Esr1*$^{f/f}$; LysMCre animals (**Figure S6E**). Myeloid cells can often manifest their actions by modulating other cell types in the TME either by facilitating the release of cytokines and/or by blunting antigen presentation to the adaptive immune cells. To understand whether T cells play a functional role in E2 induced tumor growth, we depleted CD8$^+$ T cells with an α-CD8 antibody in mice engrafted with YuMM5.2 tumor cells in the presence or absence of E2. The efficacy of the CD8$^+$ T cell depletion was confirmed by flow cytometry analysis (**Figures S6F-G**). Antibody-mediated acute depletion of CD8$^+$ T cells reversed the protective effects of ovariectomy on YuMM5.2 tumor growth but did not accelerate tumor growth in E2 treated mice (**Figure 3E**). These results suggest the functional involvement of CD8+ T cells in E2-mediated tumor growth.

To define the extent to which E2 treated myeloid cells affect T cell functionality, we isolated CD11b$^+$ myeloid cells from iBP tumors treated either with placebo or E2. These cells were then co-incubated with CD3$^+$ T cells isolated from the spleens of non-tumor bearing Pmel mice (*Thy1*^{a}/Cy Tg(TcraTcrb)8Rest/J) for 72 hrs. iBP tumors express gp100 (Pmel) (44) that can be processed and presented by professional antigen presenting cells to T cells that are specific to the antigen (gp100). Prior to coincubation, T cells were stained with the Carboxyfluorescein succinimidyl ester (CFSE) dye and activated in the presence of sub-optimal CD3/CD28. As assessed by CFSE dye dilution it was apparent that T cell (both CD4$^+$ and CD8$^+$) proliferation was significantly inhibited by co-incubation with myeloid cells isolated from tumors of E2 treated mice as compared to those T cells that were incubated with myeloid cells isolated from placebo treated mice (**Figures 3F-I**). Additionally, myeloid cells from E2 treated mice also affected the cytotoxic capability of both CD8$^+$ and CD4$^+$ T cells as demonstrated by decreased expression of IFNγ

(**Figures 3J-K and N-O**) and granzyme B (GZMB) (**Figures 3L-M and P-Q**). Taken together, these observations suggest that the ERα/E2 axis increases the immunosuppressive activities of tumor-infiltrating myeloid cells. In this experiment we did not define the phenotypic characteristics of the isolated myeloid cells i.e. bone marrow derived vs resident macrophages. However, in subsequent experiments (see below) we determined that the suppressive effects of E2 are likely mediated by macrophages that differentiate from monocytes recruited to the tumor from the bone marrow.

E2 promotes the accumulation of immune-suppressive TAMs within the tumor microenvironment

Flow cytometry was used to characterize the myeloid cells within tumors isolated from iBP mice and from mice engrafted with syngeneic tumors (B16F10), treated with either placebo or E2 (**Figure S7A**). Quantitatively the infiltration of immune cells ($CD45^+$) was similar in the two models and not impacted by treatment (**Figure S7B-C**). Qualitative assessments, however, revealed that E2 treatment decreases the ratio of intratumoral immunostimulatory M1 ($MHCII^{hi}$ $CD206^-$) macrophages to immunosuppressive M2 ($MHCII^{lo}$ $CD206^{+/hi}$) macrophages (**Figures 4A-C**). Of note, we did not see any changes in the percentage of Ly6C+/Ly6G+ MDSCs in tumors between the two treatment conditions **(Figure S7D)**. Depletion of macrophages using clodronate liposomes decreased melanoma tumor growth in E2 treated mice but was without any effect in placebo treated mice (**Figures 4D and S7E**). To demonstrate a direct effect of E2 on macrophage polarization (and function), bone marrow progenitor cells were differentiated into macrophages in the presence of M-CSF and either normal media or 30% tumor conditioned media (TCM) from B16F10 cells. The addition of tumor conditioned media allows us to partially mimic the TME where tumor derived factors influence the differentiation and polarization of macrophages (45). Following differentiation, macrophages were treated acutely with either DMSO or E2 (1 nM) and then

polarized to an M2 state by the addition of IL4. The polarized macrophages were subsequently co-cultured with sub-optimally activated T cells (CD3/CD28 and IL2) isolated from spleens of non-tumor bearing mice, for 72 hours following which they were treated with protein transport inhibitors (monensin and brefeldin) for 6 hours to prevent release of cytokines and chemokines. Flow cytometry analysis revealed that T cells which were co-incubated with either placebo or E2 (1 nM) treated macrophages in normal media (NM) did not display any change in the expression of IFNγ and GZMB. The basal expression of GZMB and IFNγ in T cells was increased significantly upon exposure to macrophages cultured in TCM. However, when T cells were co-incubated with E2 (1 nM) treated macrophages differentiated in TCM, they show a decreased expression of GZMB and IFNγ compared to T cells that were co-incubated with DMSO treated macrophages (**Figures 4E-F**). These results indicate that E2 treatment induces an immune-suppressive phenotype in tumor conditioned macrophages, which in turn suppresses the cytotoxic capabilities of T cells. However, in the absence of TCM, macrophages do not affect T cell activity even in the presence of E2.

To further explore the roles of ERα in macrophage polarization we isolated and differentiated bone marrow progenitor cells from *Esr1*$^{f/f}$ and *Esr1*$^{f/f}$;LysMCre animals to bone marrow-derived macrophages (BMDM) in NM or 30% TCM (B16F10). The differentiated BMDM from both *Esr1*$^{f/f}$ and *Esr1*$^{f/f}$;LysMCre genotypes were treated with either DMSO or E2 and then polarized to M2 macrophages by the addition of IL4 (24 hours). These macrophages were then co-incubated for 72 hours with CFSE and sub-optimally activated T cells isolated from non-tumor bearing mouse spleens. Quantification of CFSE dilution demonstrated a significant attenuation of T cell proliferation after incubating with BMDMs compared to T cells alone. No difference in the proliferation of T cells was observed when T cells were co-incubated with macrophages differentiated in NM, regardless of the genotypes of the BMDM and treatments. However, using BMDMs differentiated in TCM, a significant increase in proliferation (CFSE$^{lo/-}$), activation

(CD44^{+}D69^{+}) and cytotoxic (IFNγ^{+} and GZMB^{+}) markers was observed when T cells were incubated with BMDM derived from *Esr1*$^{f/f}$;LysMCre mice compared to *Esr1*$^{f/f}$ mice irrespective of the presence or absence of E2 (**Figures 4G-K**). These results demonstrate that the depletion of ERα in the macrophages enhances their capacity to promote proliferation of cytotoxic T cells (GZMB^{+} and IFNγ^{+}). However, in contrast to previous experiments where we have observed a decrease in GZMB and IFNγ expression in T cells upon co-incubation with E2 treated macrophages, T cells did not show similar decrease in the expression of these cytotoxic T cell markers when co-incubated with E2 treated ERα$^{f/f}$ macrophages (**Figure 4E and F vs I and K**). It may be due to differences in the underlying genetics (*Esr1*$^{f/f}$ vs WT). The importance of ERα signaling in macrophages in modulating melanoma tumor growth was further probed *in vivo* by co-injecting YuMM5.2 or B16F10 tumor cells together with BMDM (**Figure S8A**) from either *Esr1*$^{f/f}$ or *Esr1*$^{f/f}$; LysMCre mice (1:1) (**Figure 4L**) into syngeneic ovariectomized C57BL/6J mice treated placebo or E2. The tumor promoting effects of E2 were significantly compromised when tumors (YuMM5.2 and B16F10) were implanted with BMDM from *Esr1*$^{f/f}$; LysMCre animals versus *Esr1*$^{f/f}$ animals (**Figures 4M and S8B**). Taken together, these results indicate the E2/ERα signaling axis in macrophages cooperates with tumor derived factors to promote the establishment of an immune-suppressive TME that facilitates melanoma tumor growth.

Examination of the scRNA seq profiles, revealed that the CD68^{+}monocyte/TAM population from E2 treated tumors express markers that were previously reported to be selectively upregulated in TAMs vs macrophages isolated from the lungs of non-tumor bearing mice (*Trem2, Apoe, Thbs1, Spp1*) (**Figure S8C**) (46). Genes associated with inflammation and those encoding select chemokines (*Itm2b*, *C1q*) and M2 macrophages markers (*Tspo, Vegfa, Tgm2*) were also upregulated in the CD68+ cells from the E2 group (**Figure S8C**) (46). The CD68^{+} population is comprised of cells from 9 different clusters (clusters 1, 2, 3, 8, 9, 15, 16, 22 and 30) (**Figure 4N**).

Analyzing the developmental trajectories of the macrophage/monocyte populations by pseudotime analysis (**Figure S8D**) revealed several major branches representing different clusters of cells emerging from monocytes (**Figure 4O**). Among these populations, clusters 2, 3 and 16 express the monocytic markers *Cd14* (**Figure S9A**) with cluster 2 (arrow A) showing higher expression of *Ly6c2* (**Figures 4O and S9B**). The cluster 2 (arrow A) population then bifurcates into two branches, cluster 3 (arrow C) and cluster 16 (arrow B) both of which express intermediate levels of *Cx3cr1* (**Figure S9C**) but cluster 3 has higher expression of *Ccr2* (**Figure S9D**) compared to cluster 16. Thus, cluster 3 likely represents inflammatory monocytes while cluster 16 are more similar to patrolling tissue resident monocytes (47). Of note, both cluster 3 and 16 are increased in E2 treated tumors compared to placebo treatment (pseudotime block 5-10, boxed region) while the percentage of *Ly6C*^{hi} monocytes (cluster 2) remains the same between the two treatments (**Figure 4P and S9B**). Cluster 3 further proceeds to a major branching point leading to the formation of 4 different trajectories, mainly cluster 15 (arrow D), cluster 1 (arrow E), cluster 9 (arrow F) and 8, 22 and 30 (arrow G) (**Figure 4O**). Among these clusters, 1, 8, 22, 30 and 15 all express genes associated with the MHCII complex (*H2-Aa, H2-Ab, H2-Dmb1* and *H2-Eb1*) (**Figures S9E-H**). Cluster 1 and 15 additionally express inflammatory genes *Il1b* (**Figure S9I**) and likely comprises of inflammatory or “M1-like” TAMs. While cluster 1 remains unchanged, cluster 15 decreases upon E2 treatment (**Figure S9Q**). Clusters 8, 22 and 30 express inflammatory genes (*Cd72* and *Tlr2*) (**Figure S8J-K**) in addition to genes of MHCII complex, however they also express genes associated with M2 macrophages (*Mrc1*) (**Figure S8L**). While the exact functionality of these macrophage subsets is not clear, phenotypically they are analogous to the population of circulating cells of monocyte/macrophage lineage that express markers of both M1 and M2 cell phenotypes as reported previously (48). Within these clusters, cluster 8 and cluster 30 show expansion upon E2 treatment, while cluster 22 remains unchanged (**Figure S9Q**). Cluster 9 is a notable exception, which expresses markers associated with immune-suppressive phenotype (*Mrc1, Folr2, Gas6, Retnla* and *Cd163*) (**Figures 4Q and S9M-O**). This cluster also

shows higher expression of *Maf*, a gene which is required for differentiation of monocytes to macrophages (**Figure S9P**)**.** Importantly, cluster 9 shows significant expansion with E2 treatment compared to placebo (**Figure S9Q**). This observation supports our hypothesis that E2 treatment leads to the expansion of macrophages that demonstrate immune-suppressive phenotypes. Taken together, this analysis suggests that E2 may promote the initial recruitment of monocytes, as evidenced by increase in cluster 3 to the tumor microenvironment where the monocytes exposed to tumor derived factors and E2 undergo faster rates of differentiation and polarization to M2 macrophages (cluster 9) while at the same time suppresses expansion of M1 macrophages (cluster 15). This result is further supported by our flow cytometry data where we observed a trend towards an increase in the number of monocytes in response to E2 (**Figure S9R**) and a decrease in M1/M2 ratio with the total number of $F480^{+}$ macrophages remaining unchanged (**Figures 4A-B and S9S**).

To determine the molecular pathway(s) that influence this M2 phenotype in E2 treated macrophages, we performed upstream regulator analysis of differentially expressed genes (DEGs) in CD68+ cells using Ingenuity Pathway Analysis (IPA). This analysis highlighted the importance of the TCF4 and WNT5A pathways (**Figure S10A-B)** the significance of which we explored in tumor infiltrating myeloid cells isolated from iBP tumors excised from mice treated with placebo or E2. Gene expression analysis revealed that multiple genes in the WNT5A and TCF4 pathways were differentially regulated by E2 compared to placebo in these cells (**Figure S10C**). WNT5A, signaling through the canonical β-catenin pathway, has been implicated in various biological processes including embryogenesis, cell fate development, and endothelial cell differentiation resulting in the upregulation of vasculogenic and angiogenic processes, although the significance of E2 in the regulation of these processes in the TME remains to be determined. Of note, WNT5A signaling has also been reported to induce tolerogenic phenotypes in macrophages in breast cancer patients (49). We demonstrate that myeloid cells isolated from E2 treated tumors manifest a gene expression pattern characteristic of M2 macrophages with

increased expression of multiple genes, such as *Vegfa*, *Tgm2* and *Tspo* and *Stat1* (50-52) (**Figure S10D**). It has yet to be determined whether E2-regulated expression of these genes depends on WNT signaling. In contrast to myeloid cells, knockdown of *Esr1* or treatment with either E2 (1nM) or E2 (1nM)+fulvestrnat (100nM) did not change the expression of WNT5A-β-catenin targets in YuMM5.2 cells (**Figure S10E-F**) although E2/ER signaling has previously been shown to influence β-catenin signaling in cancer cells (53). Together, these results indicate a likely role for E2 in the functional activation of WNT5A-β-catenin signaling leading to macrophage polarization towards an immune-suppressive state in the melanoma tumor microenvironment.

E2 treatment suppresses anti-tumor T cell responses

The results of the *ex vivo* studies described above suggested that E2 exerts a direct effect on macrophages to suppress the proliferation and activity of both $CD4^+$ and $CD8^+$ T cells. Flow cytometry analysis of tumor-infiltrating T cells from iBP tumors also revealed an overall decrease in the $CD3^+$ T cell population with E2 treatment (**Figures 5A-B and S11A**). Further, sub-gating of the $CD3^+$ positive T cell population indicated that the number of intra-tumoral $CD8^+$ cytotoxic T cells were decreased upon E2 treatment, while no significant changes in $CD4^+$ T cells were observed (**Figures 5C-D and Figures S11B-C**). We also evaluated the activity of tumor infiltrating T cells using $CD3^+$ T cells isolated from syngeneic YuMM5.2 tumors. For this purpose, T cells were isolated from placebo and E2 treated tumors and *ex vivo* treated with PMA and ionomycin for 4 hours along with protein transport inhibitors. Flow cytometry analysis demonstrated that when compared to T cells isolated from placebo treated mice, the $CD8^+$ tumor infiltrating lymphocytes (TILs) isolated from E2 treated YuMM5.2 tumors were markedly more exhausted, expressing significantly more PD1 (**Figures 5E-F**) and reduced expression of Granzyme B, (**Figures 5G-H**), activation markers CD44 and CD69 (**Figures 5I-J**), and cytokines such as IFNγ (**Figures 5K-L**). As in the iBP model we did not observe a significant impact of E2 treatment on the infiltration of $CD4^+$ $FOXP3^+$ regulatory T cell subsets (**Figures S11D-E**). When taken together,

these results suggest that systemic E2 treatment reduces T cell functionality albeit in an indirect manner as *Esr1, Esr2 or Gper1* RNA were not expressed in T cells within the tumor microenvironment (**Figures S5B-D**). Further, treatment of T cells *in vitro* with either E2 or the SERD fulvestrant did not affect the proliferation or cytotoxic capabilities of either $CD4^+$ or $CD8^+$ T cells (**Figures S12A-J**). Taken together, these data indicate that E2 indirectly reduces T cell function secondary to its effects on macrophages.

Pharmacological inhibition of ER reverses the growth promoting effects of E2 on melanoma tumors

Fulvestrant, a SERD, acts by both inactivating and degrading ER and is approved for use in post-menopausal patients with ER-positive breast cancer who have progressed on first-line endocrine therapies (54). It was selected for these studies as it is the most efficacious ER inhibitor currently available for clinical use (55). At a dose that we have determined to model achievable levels in breast cancer patients (25mg/kg) (56), fulvestrant significantly reduced tumor growth in all preclinical models of melanoma examined (B16F10, YuMM5.2 and BPD6) (**Figures 6A-C, S13A-C**). To understand how fulvestrant affects the TME, we analyzed the tumor infiltrating immune cell repertoire by flow cytometry. We observed an increase in intratumoral M1/M2 ratio or an increase in inflammatory macrophages ($MHCII^{hi}$ $CD206^-$), when E2 treated mice were co-treated with fulvestrant (**Figures 6D, E and S13D-E**). Tumor infiltrating T cells from fulvestrant treated tumors displayed an increase in cytotoxic capabilities as measured by Granzyme B (GZMB) expression (**Figure 6F**). Additionally, fulvestrant treatment led to a decrease in the number of $PD1^+CD8^+$T cells (exhausted T cells) that increased with E2 treatment **(Figure 6G**). Similar observations were made in studies performed *in vitro* when BMDM cells treated with fulvestrant were co-incubated with CFSE-labelled sub-optimally activated (CD3/CD28) T cells in presence of IL2. Analysis of CFSE dilution revealed that the proliferation of T cells was not affected by their co-incubation with macrophages differentiated in NM and treated with either E2 or E2+fulvestrant. However, T cells

exposed to macrophages, differentiated in 30% TCM and E2, effectively suppressed T cell proliferation, an activity that was reversed by treatment with fulvestrant (**Figure S13F**). Collectively, these results indicate that fulvestrant can inhibit the effects of E2 on tumor growth and remodel the tumor immune microenvironment to favor tumor growth inhibition in melanoma.

We next undertook studies to evaluate whether fulvestrant improves/restores response to the immune checkpoint inhibitor, α-PD1, in the PD1 sensitive BPD6 and unresponsive B16F10 tumor model. In the PD1 sensitive BPD6 model, treatment with either fulvestrant or ICB (α-PD1 and α-CTLA4) slows tumor growth, however the combination of both drugs further suppressed tumor growth when compared to each individual treatment (**Figures 6H and I**). To determine whether fulvestrant can also increase the effectiveness of immunotherapy in ICB unresponsive B16F10 model, we treated mice with established B16F10 tumors with fulvestrant and α- PD1 either alone or in combination. Importantly, the combination of fulvestrant with α-PD1 suppressed the growth of B16F10 tumors, while PD1 treatment alone was without any effect (**Figures 6J-L**). Taken together these results indicate that pharmacological targeting of ERα can improve the intratumoral M1/M2 ratio and increase the effectiveness of ICB in both ICB sensitive and resistant models of melanoma. Since E2-driven tumor growth appears to be macrophage dependent, we anticipated that a macrophage specific ERα signature would predict ICB sensitivity in melanoma patients. To this end, we first divided the E2-regulated genes in all $CD68^{+}$ macrophage/monocyte clusters identified from scRNA seq into 2 groups: genes upregulated by E2 (E2-Up response) and genes down regulated by E2 (E2-Down response) (**Supplementary File II**). We then used the human orthologs of the identified murine signatures to predict survival of patients receiving ICB treatments using publicly available transcriptional datasets from patients receiving ICB treatments (32). We observed that an enrichment of macrophage specific-E2 down regulated genes (E2-Down) correlated with a better overall survival in melanoma patients who have received ICB (**Figure 6M**). These results highlight the importance of ERα function in TAMs residing in

melanoma TME and demonstrate how an ERα specific signature can be utilized to predict a patient's response to ICB treatments.

Discussion

We have identified a tumor cell extrinsic activity of ERα that results in an increased accumulation of M2 or alternatively activated macrophages in the TME that suppresses adaptive immunity and promotes tumor growth in murine models of melanoma. Previously, it has been demonstrated that E2 promotes MDSC mobilization to tumor sites and creates an immune-suppressive tumor microenvironment in ovarian, lung and breast cancer (22). While there is anecdotal evidence suggesting that elevated numbers of circulating monocytic MDSCs track with Ipilimumab treatment outcome in melanoma patients (57), our data reveal that it is the intratumoral M1/M2 macrophage ratio, and not changes in granulocytic MDSCs, that predicts responses in patients treated with either PD1 or CTLA4 alone or in combination. This encouraged us to investigate the mechanisms by which E2 modulates response to ICBs. Here we provide evidence that removal of endogenous estrogens (ovariectomy) provides a protective advantage against tumor growth in part by decreasing the number of immune suppressive TAMs and by preventing the exhaustion of cytotoxic T cells. This function was primarily attributed to E2/ER signaling in macrophages and their ability to facilitate M2 polarization. Of clinical importance is the finding that the SERD, fulvestrant, can reverse the effects of E2 on tumor growth and immune cell repertoire, establishing the importance of ER in melanoma biology and highlighting a potential new treatment modality for this disease.

Tumor associated macrophages are one of the dominant immune cell types within the TME and can promote tumor growth by increasing neo-vascularization, promoting wound healing/tissue repair processes and blocking the activation of adaptive immune cells within the TME (58-60). TAM recruitment in tumors is generally associated with resistance to chemotherapy and immunotherapy and thus there is a high level of interest in developing interventional approaches to suppress the immune-suppressive and pro-tumoral activities of these cells (60-63). Among the

strategies employed and/or under investigation are depletion of TAMs in the TME using CSF1R antibodies (64, 65) or bisphosphonates (66-68); prevention of TAM recruitment to tumors by inhibiting the CCL2/CCR2 axis (69-71) or reprogramming of TAMs using anti-CD47-SIRPα antibodies, TLR agonists and inhibitors of the enzyme calcium calmodulin kinase kinase-2 (72-75). While somewhat successful in different tumor contexts, these therapies have often suffered from severe toxicities that have limited their use in patients. This highlights the potential clinical importance of our observation that estrogens (E2) can promote the establishment and maintenance of a tumor suppressive microenvironment by TAM polarization- an activity that can be reversed by ER antagonist/SERD, fulvestrant.

Estrogens have been shown to play a major role in reducing inflammation by promoting the polarization of macrophages towards an anti-inflammatory state during airway inflammation and cutaneous wound repair (19, 21). However, very little is known as to how E2 effects TAM function in tumors. In breast and ovarian cancer, tumor cell intrinsic E2/ER signaling has been linked to increased recruitment of TAMs in the tumor microenvironment (76-78). Our study, on the other hand, highlighted a specific role for TAM intrinsic E2/ER signaling in promoting tumor growth in validated murine models of melanoma. We have demonstrated that inhibition of estrogen action in macrophages (depletion of ER) can recapitulate the systemic depletion of estrogen action on melanoma tumor growth. Therefore, it appears that most of the protumorigenic actions of E2 in the melanoma tumor microenvironment can be attributed to ER signaling in macrophages.

One of the most important findings in this study was that E2 polarized TAMs within the TME display the phenotypic features of M2-like immunosuppressive macrophages. This observation was confirmed by both flow cytometry analysis and by pseudotime analysis of gene expression from single cell RNA sequencing data, in which it was revealed that E2 leads to an initial accumulation of both inflammatory and patrolling monocytes. It then accelerates the polarization of inflammatory monocytes to M2 macrophages that express characteristic immune-suppressive

markers (*Cd163, Mrc1, Folr2, Retnla and Gas6*). However, the molecular mechanism(s) underlying this accelerated polarization of monocytes to macrophages remain to be determined. The functional significance of an increased accumulation of immunosuppressive macrophages was highlighted by demonstrating that E2 treated TAMs blocked the cytotoxic activity of $CD8^+$ T cells by preventing granzyme B expression and IFNγ release. Importantly, this activity was only manifested by macrophages residing in the tumor microenvironment and in BMDM cultured in TCM but not observed in BMDM cultured in NM. These results indicate that soluble factors secreted by tumor cells work in concert with E2 to promote TAM polarization that subsequently suppresses adaptive immunity. In line with that, we have observed changes in the expression of targets downstream of WNT5A/TCF4 signaling in tumor associated myeloid cells treated with E2. Although functioning primarily as a positive regulator of the non-canonical WNT signaling pathway, WNT5A can in some contexts activate canonical WNT signaling through β-catenin to increase TCF/LEF transcriptional activity (79). Importantly, it has been demonstrated that tumor cell derived WNT5A can induce β-catenin activation in DCs leading to enhanced Indoleamine 2, 3 dioxygenase (IDO) production, melanoma progression and M2 polarization (80). Since we have observed E2-mediated regulation of WNT5A targets in tumor associated myeloid cells, we speculate that tumor derived WNT5A may work in collaboration with E2 to skew macrophage polarization towards an immune-suppressive state and suppress T cell activity.

In contrast to $CD8^+$ T cells, we observed varying effects of E2 on $CD4^+$ T cell activation and/or proliferation when co-culturing with macrophages *in vitro* vs $CD4^+$ T cells in E2 treated tumors *in vivo*. While *in vitro* activated $CD4^+$ T cells from naïve mice, co-cultured with myeloid cells isolated from E2 treated tumors *ex vivo,* demonstrate a decrease in proliferative and cytotoxic capabilities, there were no apparent differences in either proliferation or cytotoxicity of $CD4^+$ T cells in placebo or E2 treated tumors. Apart from TAMs, the $CD4^+$ T cells in the tumors are chronically exposed to cytokines and factors secreted by different cell types residing in the tumor which may account

for lack of differences in their proliferative and cytotoxic states between placebo and E2; a possibility we are currently exploring.

ERα modulators are used as first-line treatment in ER+ breast cancer where tumor cell intrinsic actions of E2/ER axis facilitate tumor growth (81). Our data demonstrates that in hormone-independent cancers (i.e., no direct effects of estrogens on cancer cells) like melanoma, ER antagonists/SERDs, such as fulvestrant, can efficiently suppress tumor growth by promoting anti-tumor immunity. The results of studies using tamoxifen in melanoma patients were equivocal (82, 83), likely attributable to its inherent partial ER-agonistic activity. Fulvestrant is both a high affinity competitive antagonist and a receptor degrader allowing for a deep inhibition of ER action (84). Unfortunately, although an approved drug, its poor pharmaceutical properties has limited the clinical use of fulvestrant (85). Currently, there are twelve new orally bioavailable SERDs in clinical development, and we have an ongoing interest in evaluating the potential utility of these drugs as immune modulators. Moreover, useful cell/process selective ER inhibition can also be achieved using Selective Estrogen Receptor Modulators (SERMs) (i.e. bazedoxifene, lasofoxifene and raloxifene), drugs whose relative agonist/antagonist properties differ depending on cell/tissue context (86). Thus, in addition to profiling new SERDs, our studies provide the rationale for testing different classes of SERDs and SERMs for their ability to reprogram macrophage function and increase tumor immunity in the setting of melanoma.

One of the most important findings of this study is that fulvestrant works in concert with ICBs to suppress melanoma tumor growth in both ICB sensitive and ICB unresponsive syngeneic models of melanoma. This can be attributed, at least in part, to the ability of fulvestrant to promote a pro immunogenic environment by elevating the M1 to M2 macrophage ratio and by increasing the number of intratumoral activated $CD8^+$ T cells. This observation has significant clinical importance as although α-PD1 therapy is successful in some melanoma patients, the majority of treated patients do not respond to, or acquire resistance to, this intervention. We believe that the findings in murine models of melanoma will translate to humans. This position is supported by our findings

that a macrophage-derived, ER-downregulated, gene signature can predict survival in melanoma patients treated with ipilimumab and pembrolizumab/nivolumab (32). These findings highlight the potential clinical utility of using a combination of ER modulators (SERDs or SERMs) with ICBs in melanoma patients who develop ICB resistance due to an increased accumulation of immune suppressive TAMs in tumors (34, 87). Additionally, we demonstrate that expression of the aromatase gene, correlates with enhanced expression of TAM markers such as *CD68*, *CSF1R*, *CSF1,* as well as a trend towards increased expression of *PDCD1* in α-PD1 non-responders. This finding suggests that although patients who have higher levels of circulating estrogens are particularly vulnerable to develop resistance to α-PD1 therapy that intra-tumoral E2 production may also contribute to disease pathobiology. One of the major side effects of ICBs is the development of immune related adverse events (irAE), among which endocrine toxicities are most frequent. While the most common endocrinopathies related to ICB usage is associated with thyroid dysfunction, recent reports have also suggested a significant increase in risk of hypogonadism in ICB treated patients (88, 89). Thus, the use of appropriate SERMs that demonstrate estrogenic action towards reproductive organs to ameliorate the inflammatory side effects of ICB, while at the same time promoting anti-tumor immunity, may have added clinical utility.

In conclusion, we have demonstrated that the E2/ER axis plays an important role in macrophage reprogramming within the melanoma TME and that specific targeting of the ER signaling axis in macrophages may improve the long-term survival of melanoma patients. While we have provided extensive evidence describing the role of ERα in modulating TAM polarization and suppression of adaptive immunity, the exact mechanism(s) by which E2 influences the immune suppressive activity of the TAM remain to be determined. Future studies addressing the possible mechanisms by which E2 influences TAM biology will be informative as to which of the existing SERMs or SERDs will be most useful for use in ICB regimens and/or help to define the characteristics of

next generation ER-modulators optimized for their positive effects on tumor immunity. Additionally, while our study exclusively focusses on TAM intrinsic E2/ER signaling, others have shown that melanoma cells express both nuclear ERs (ERα and ERβ) (90) as well as GPER (16). While the functionality of these receptors in melanoma cells are yet to be studied in detail, we cannot completely rule out the contribution of melanoma cell intrinsic E2/ER signaling to the tumor growth phenotype we have observed. Studies using melanoma cells genetically depleted of ER will be informative as to the contribution of tumor cell intrinsic E2/ER signaling on melanoma biology.

Taken together, the results of our studies have provided the underlying rationale for a clinical study we are about to undertake to explore the use of fulvestrant (and potentially other ER-modulators) as a means to increase the efficacy of immune checkpoint inhibitors.

Methods

Mice: C57BL/6J, LysMCre (B6.129P2-*Lyz2*$^{tm1(cre)Ifo}$/J)(91) Pmel (B6.Cg-*Thy1*^{a} /Cy Tg(TcraTcrb)8Rest/J) (92) mice were purchased from Jackson Laboratories (Bar Harbor, ME). Age matched mice were used for all the studies. LysMCre mice were bred to *Esr1*$^{f/f}$ mice (a gift from Dr. Ken Korach, NIEHS) to generate *Esr1*$^{f/f}$;LysMCre and littermate control LysMCre and *Esr1*$^{f/f}$ mice. iBP (Braf$^{V600E/WT}$,Pten$^{f/f}$ mTyrCreERT2) mice were generated by crossing breeders Braf$^{WT/WT}$/*Pten*$^{f/f}$,mTyrCreERT2 mice to BRAF^{V600E}, *Pten*$^{f/f}$ mice. The mice were housed in secure animal facility cages in 12hrs light:dark cycles at temperature around 25°C and 70% humidity. Mice had access to ad-libitum food and water. NSG (NOD.Cg-*Prkdc*^{scid} *Il2rg*^{tm1Wjl}/SzJ) were purchased from the Division of Laboratory Animal Resources (Duke University). The NSG animals were fed with a GL3 diet and were kept in pathogen free conditions.

Tumor models and cells. The mouse B16F10 and Yumm5.2 cell lines were purchased from American Type Culture Collection (ATCC, Manassas, VA). The mouse melanoma cell line BPD6 was established from iBP as described elsewhere (80). The details of the culture conditions and tumor models are described in supplemental methods.

Ovariectomy and subcutaneous pellet insertion. Ovariectomy was performed as detailed in (93). Details of ovariectomy are discussed in supplemental methods.

Single Cell RNA sequencing: iBP tumors (three) were pooled and a single cell suspension was isolated as described in the Supplemental method section. Live, tumor infiltrating immune cells ($CD45^{+}$ L/D^{-}) were isolated by cell sorting and resuspended in PBS+0.04% BSA at a concentration of 1000 cells/µl. Details of the single cell RNA sequencing experiment and its analysis are outlined in supplemental methods.

Statistics: Statistics was performed, using GraphPad Prism 8.0 software, by either two-tailed Student's T test, one-way ANOVA or two-way ANOVA as indicated in the legends. For both one-way and two-way ANOVA, post-test analysis was performed using Bonferroni's multiple correction. Number of replicates are provided in the legends of the figures. Level of significance was determined to be $p < 0.05$.

Study approval

All animal experiments were performed according to guidelines from and approved by the Duke Institutional Animal Care and Use Committee (IACUC).

Data Availability: Raw data for scRNA seq has been deposited in Gene Expression Omnibus under the accession number GSE171403.

Author Contribution

B.C, C.Y.C and D.P.M conceived of and designed all of the experiments. B.C, J.B C.Y.C, R.B, W.L, D.M, S.A, O.B, K.T and Y.B. J.S performed the experimental work. W.G, C.H and CP performed the analysis of scRNA sequencing data and the analysis of human correlates. Manuscript was written by B.C and D.P.M with critical inputs from C.Y.C and C.H. The project was managed and overseen by CYC and D.P.M.

Acknowledgements: We would like to thank Dr. Xia Gao for critical reading of our manuscript. We would like to acknowledge the assistance of the Duke Molecular Physiology Institute Molecular Genomics core for the generation of scRNA sequencing data for the manuscript. This project was supported (in part) by a Melanoma Research Foundation Grant (640233), Susan G

Komen Foundation grant (SAC180085), and Duke Cancer Institute pilot funding grant to D.P.M and a Susan G Komen Foundation grant (SAC160074) to C.P.

Conflict of Interest: The authors have declared that no conflict of interest exists.

References

1. Gogas HJ, Kirkwood JM, and Sondak VK. Chemotherapy for metastatic melanoma: time for a change? *Cancer.* 2007;109(3):455-64.
2. Chapman PB, Hauschild A, Robert C, Haanen JB, Ascierto P, Larkin J, et al. Improved survival with vemurafenib in melanoma with BRAF V600E mutation. *The New England journal of medicine.* 2011;364(26):2507-16.
3. Robert C, Long GV, Brady B, Dutriaux C, Maio M, Mortier L, et al. Nivolumab in previously untreated melanoma without BRAF mutation. *The New England journal of medicine.* 2015;372(4):320-30.
4. Topalian SL, Sznol M, McDermott DF, Kluger HM, Carvajal RD, Sharfman WH, et al. Survival, durable tumor remission, and long-term safety in patients with advanced melanoma receiving nivolumab. *Journal of clinical oncology : official journal of the American Society of Clinical Oncology.* 2014;32(10):1020-30.
5. Hodi FS, O'Day SJ, McDermott DF, Weber RW, Sosman JA, Haanen JB, et al. Improved survival with ipilimumab in patients with metastatic melanoma. *The New England journal of medicine.* 2010;363(8):711-23.
6. Larkin J, Chiarion-Sileni V, Gonzalez R, Grob JJ, Cowey CL, Lao CD, et al. Combined Nivolumab and Ipilimumab or Monotherapy in Untreated Melanoma. *The New England journal of medicine.* 2015;373(1):23-34.
7. Sosa A, Lopez Cadena E, Simon Olive C, Karachaliou N, and Rosell R. Clinical assessment of immune-related adverse events. *Ther Adv Med Oncol.* 2018;10:1758835918764628.
8. Sadoff L, Winkley J, and Tyson S. Is malignant melanoma an endocrine-dependent tumor? The possible adverse effect of estrogen. *Oncology.* 1973;27(3):244-57.
9. Schmidt AN, Nanney LB, Boyd AS, King LE, Jr., and Ellis DL. Oestrogen receptor-beta expression in melanocytic lesions. *Exp Dermatol.* 2006;15(12):971-80.
10. Mitkov M, Joseph R, and Copland J, 3rd. Steroid hormone influence on melanomagenesis. *Mol Cell Endocrinol.* 2015;417:94-102.
11. Moller H, Purushotham A, Linklater KM, Garmo H, Holmberg L, Lambe M, et al. Recent childbirth is an adverse prognostic factor in breast cancer and melanoma, but not in Hodgkin lymphoma. *European journal of cancer.* 2013;49(17):3686-93.
12. Holly EA, Cress RD, and Ahn DK. Cutaneous melanoma in women: ovulatory life, menopause, and use of exogenous estrogens. *Cancer epidemiology, biomarkers & prevention : a publication of the American Association for Cancer Research, cosponsored by the American Society of Preventive Oncology.* 1994;3(8):661-8.
13. Huber C, Bouchardy C, Schaffar R, Neyroud-Caspar I, Vlastos G, Le Gal FA, et al. Antiestrogen therapy for breast cancer modifies the risk of subsequent cutaneous melanoma. *Cancer Prev Res (Phila).* 2012;5(1):82-8.
14. Conforti F, Pala L, Bagnardi V, De Pas T, Martinetti M, Viale G, et al. Cancer immunotherapy efficacy and patients' sex: a systematic review and meta-analysis. *Lancet Oncol.* 2018;19(6):737-46.
15. Khan D, and Ansar Ahmed S. The Immune System Is a Natural Target for Estrogen Action: Opposing Effects of Estrogen in Two Prototypical Autoimmune Diseases. *Frontiers in immunology.* 2015;6:635.
16. Natale CA, Li J, Zhang J, Dahal A, Dentchev T, Stanger BZ, et al. Activation of G protein-coupled estrogen receptor signaling inhibits melanoma and improves response to immune checkpoint blockade. *eLife.* 2018;7.

17. Dika E, Patrizi A, Lambertini M, Manuelpillai N, Fiorentino M, Altimari A, et al. Estrogen Receptors and Melanoma: A Review. *Cells.* 2019;8(11).
18. Pequeux C, Raymond-Letron I, Blacher S, Boudou F, Adlanmerini M, Fouque MJ, et al. Stromal estrogen receptor-alpha promotes tumor growth by normalizing an increased angiogenesis. *Cancer research.* 2012;72(12):3010-9.
19. Keselman A, Fang X, White PB, and Heller NM. Estrogen Signaling Contributes to Sex Differences in Macrophage Polarization during Asthma. *J Immunol.* 2017;199(5):1573-83.
20. Straub RH. The complex role of estrogens in inflammation. *Endocr Rev.* 2007;28(5):521-74.
21. Campbell L, Emmerson E, Williams H, Saville CR, Krust A, Chambon P, et al. Estrogen receptor-alpha promotes alternative macrophage activation during cutaneous repair. *J Invest Dermatol.* 2014;134(9):2447-57.
22. Svoronos N, Perales-Puchalt A, Allegrezza MJ, Rutkowski MR, Payne KK, Tesone AJ, et al. Tumor Cell-Independent Estrogen Signaling Drives Disease Progression through Mobilization of Myeloid-Derived Suppressor Cells. *Cancer Discov.* 2017;7(1):72-85.
23. Dysthe M, and Parihar R. Myeloid-Derived Suppressor Cells in the Tumor Microenvironment. *Adv Exp Med Biol.* 2020;1224:117-40.
24. Nalbandian G, Paharkova-Vatchkova V, Mao A, Nale S, and Kovats S. The selective estrogen receptor modulators, tamoxifen and raloxifene, impair dendritic cell differentiation and activation. *Journal of immunology.* 2005;175(4):2666-75.
25. Pelekanou V, Kampa M, Kiagiadaki F, Deli A, Theodoropoulos P, Agrogiannis G, et al. Estrogen anti-inflammatory activity on human monocytes is mediated through cross-talk between estrogen receptor ERalpha36 and GPR30/GPER1. *J Leukoc Biol.* 2016;99(2):333-47.
26. Fujiwara T, Fukushi J, Yamamoto S, Matsumoto Y, Setsu N, Oda Y, et al. Macrophage infiltration predicts a poor prognosis for human ewing sarcoma. *The American journal of pathology.* 2011;179(3):1157-70.
27. Mahmoud SM, Lee AH, Paish EC, Macmillan RD, Ellis IO, and Green AR. Tumour-infiltrating macrophages and clinical outcome in breast cancer. *J Clin Pathol.* 2012;65(2):159-63.
28. Yagi T, Baba Y, Okadome K, Kiyozumi Y, Hiyoshi Y, Ishimoto T, et al. Tumour-associated macrophages are associated with poor prognosis and programmed death ligand 1 expression in oesophageal cancer. *European journal of cancer.* 2019;111:38-49.
29. Ryder M, Ghossein RA, Ricarte-Filho JC, Knauf JA, and Fagin JA. Increased density of tumor-associated macrophages is associated with decreased survival in advanced thyroid cancer. *Endocr Relat Cancer.* 2008;15(4):1069-74.
30. Bronkhorst IH, Ly LV, Jordanova ES, Vrolijk J, Versluis M, Luyten GP, et al. Detection of M2-macrophages in uveal melanoma and relation with survival. *Invest Ophthalmol Vis Sci.* 2011;52(2):643-50.
31. Hasita H, Komohara Y, Okabe H, Masuda T, Ohnishi K, Lei XF, et al. Significance of alternatively activated macrophages in patients with intrahepatic cholangiocarcinoma. *Cancer Sci.* 2010;101(8):1913-9.
32. Gide TN, Quek C, Menzies AM, Tasker AT, Shang P, Holst J, et al. Distinct Immune Cell Populations Define Response to Anti-PD-1 Monotherapy and Anti-PD-1/Anti-CTLA-4 Combined Therapy. *Cancer Cell.* 2019;35(2):238-55 e6.
33. Van Allen EM, Miao D, Schilling B, Shukla SA, Blank C, Zimmer L, et al. Genomic correlates of response to CTLA-4 blockade in metastatic melanoma. *Science.* 2015;350(6257):207-11.
34. Hugo W, Zaretsky JM, Sun L, Song C, Moreno BH, Hu-Lieskovan S, et al. Genomic and Transcriptomic Features of Response to Anti-PD-1 Therapy in Metastatic Melanoma. *Cell.* 2016;165(1):35-44.

35. Charoentong P, Finotello F, Angelova M, Mayer C, Efremova M, Rieder D, et al. Pan-cancer Immunogenomic Analyses Reveal Genotype-Immunophenotype Relationships and Predictors of Response to Checkpoint Blockade. *Cell reports.* 2017;18(1):248-62.
36. Youn JI, Collazo M, Shalova IN, Biswas SK, and Gabrilovich DI. Characterization of the nature of granulocytic myeloid-derived suppressor cells in tumor-bearing mice. *J Leukoc Biol.* 2012;91(1):167-81.
37. Schlecker E, Stojanovic A, Eisen C, Quack C, Falk CS, Umansky V, et al. Tumor-infiltrating monocytic myeloid-derived suppressor cells mediate CCR5-dependent recruitment of regulatory T cells favoring tumor growth. *Journal of immunology.* 2012;189(12):5602-11.
38. Bindea G, Mlecnik B, Tosolini M, Kirilovsky A, Waldner M, Obenauf AC, et al. Spatiotemporal dynamics of intratumoral immune cells reveal the immune landscape in human cancer. *Immunity.* 2013;39(4):782-95.
39. Newman AM, Liu CL, Green MR, Gentles AJ, Feng W, Xu Y, et al. Robust enumeration of cell subsets from tissue expression profiles. *Nat Methods.* 2015;12(5):453-7.
40. Ye Y, Jing Y, Li L, Mills GB, Diao L, Liu H, et al. Sex-associated molecular differences for cancer immunotherapy. *Nature communications.* 2020;11(1):1779.
41. Marzagalli M, Montagnani Marelli M, Casati L, Fontana F, Moretti RM, and Limonta P. Estrogen Receptor beta in Melanoma: From Molecular Insights to Potential Clinical Utility. *Front Endocrinol (Lausanne).* 2016;7:140.
42. Rajabi P, Bagheri M, and Hani M. Expression of Estrogen Receptor Alpha in Malignant Melanoma. *Adv Biomed Res.* 2017;6:14.
43. Dankort D, Curley DP, Cartlidge RA, Nelson B, Karnezis AN, Damsky WE, Jr., et al. Braf(V600E) cooperates with Pten loss to induce metastatic melanoma. *Nature genetics.* 2009;41(5):544-52.
44. Kohler C, Nittner D, Rambow F, Radaelli E, Stanchi F, Vandamme N, et al. Mouse Cutaneous Melanoma Induced by Mutant BRaf Arises from Expansion and Dedifferentiation of Mature Pigmented Melanocytes. *Cell Stem Cell.* 2017;21(5):679-93 e6.
45. Benner B, Scarberry L, Suarez-Kelly LP, Duggan MC, Campbell AR, Smith E, et al. Generation of monocyte-derived tumor-associated macrophages using tumor-conditioned media provides a novel method to study tumor-associated macrophages in vitro. *J Immunother Cancer.* 2019;7(1):140.
46. Lavin Y, Kobayashi S, Leader A, Amir ED, Elefant N, Bigenwald C, et al. Innate Immune Landscape in Early Lung Adenocarcinoma by Paired Single-Cell Analyses. *Cell.* 2017;169(4):750-65 e17.
47. Yang J, Zhang L, Yu C, Yang XF, and Wang H. Monocyte and macrophage differentiation: circulation inflammatory monocyte as biomarker for inflammatory diseases. *Biomark Res.* 2014;2(1):1.
48. Trombetta AC, Soldano S, Contini P, Tomatis V, Ruaro B, Paolino S, et al. A circulating cell population showing both M1 and M2 monocyte/macrophage surface markers characterizes systemic sclerosis patients with lung involvement. *Respir Res.* 2018;19(1):186.
49. Bergenfelz C, Medrek C, Ekstrom E, Jirstrom K, Janols H, Wullt M, et al. Wnt5a induces a tolerogenic phenotype of macrophages in sepsis and breast cancer patients. *Journal of immunology.* 2012;188(11):5448-58.
50. Yang P, Yu D, Zhou J, Zhuang S, and Jiang T. TGM2 interference regulates the angiogenesis and apoptosis of colorectal cancer via Wnt/beta-catenin pathway. *Cell Cycle.* 2019;18(10):1122-34.
51. Wolf A, Herb M, Schramm M, and Langmann T. The TSPO-NOX1 axis controls phagocyte-triggered pathological angiogenesis in the eye. *Nature communications.* 2020;11(1):2709.
52. Battle TE, Lynch RA, and Frank DA. Signal transducer and activator of transcription 1 activation in endothelial cells is a negative regulator of angiogenesis. *Cancer research.* 2006;66(7):3649-57.

53. Liu S, Fan W, Gao X, Huang K, Ding C, Ma G, et al. Estrogen receptor alpha regulates the Wnt/beta-catenin signaling pathway in colon cancer by targeting the NOD-like receptors. *Cell Signal.* 2019;61:86-92.
54. Nathan MR, and Schmid P. A Review of Fulvestrant in Breast Cancer. *Oncol Ther.* 2017;5(1):17-29.
55. Robertson JF, Llombart-Cussac A, Rolski J, Feltl D, Dewar J, Macpherson E, et al. Activity of fulvestrant 500 mg versus anastrozole 1 mg as first-line treatment for advanced breast cancer: results from the FIRST study. *J Clin Oncol.* 2009;27(27):4530-5.
56. Wardell SE, Yllanes AP, Chao CA, Bae Y, Andreano KJ, Desautels TK, et al. Pharmacokinetic and pharmacodynamic analysis of fulvestrant in preclinical models of breast cancer to assess the importance of its estrogen receptor-alpha degrader activity in antitumor efficacy. *Breast cancer research and treatment.* 2020;179(1):67-77.
57. Meyer C, Cagnon L, Costa-Nunes CM, Baumgaertner P, Montandon N, Leyvraz L, et al. Frequencies of circulating MDSC correlate with clinical outcome of melanoma patients treated with ipilimumab. *Cancer Immunol Immunother.* 2014;63(3):247-57.
58. Ostuni R, Kratochvill F, Murray PJ, and Natoli G. Macrophages and cancer: from mechanisms to therapeutic implications. *Trends Immunol.* 2015;36(4):229-39.
59. Cassetta L, and Pollard JW. Targeting macrophages: therapeutic approaches in cancer. *Nature reviews Drug discovery.* 2018;17(12):887-904.
60. Petty AJ, and Yang Y. Tumor-associated macrophages: implications in cancer immunotherapy. *Immunotherapy.* 2017;9(3):289-302.
61. DeNardo DG, Brennan DJ, Rexhepaj E, Ruffell B, Shiao SL, Madden SF, et al. Leukocyte complexity predicts breast cancer survival and functionally regulates response to chemotherapy. *Cancer discovery.* 2011;1(1):54-67.
62. Arlauckas SP, Garris CS, Kohler RH, Kitaoka M, Cuccarese MF, Yang KS, et al. In vivo imaging reveals a tumor-associated macrophage-mediated resistance pathway in anti-PD-1 therapy. *Sci Transl Med.* 2017;9(389).
63. Gordon SR, Maute RL, Dulken BW, Hutter G, George BM, McCracken MN, et al. PD-1 expression by tumour-associated macrophages inhibits phagocytosis and tumour immunity. *Nature.* 2017;545(7655):495-9.
64. Tap WD, Wainberg ZA, Anthony SP, Ibrahim PN, Zhang C, Healey JH, et al. Structure-Guided Blockade of CSF1R Kinase in Tenosynovial Giant-Cell Tumor. *The New England journal of medicine.* 2015;373(5):428-37.
65. Butowski N, Colman H, De Groot JF, Omuro AM, Nayak L, Wen PY, et al. Orally administered colony stimulating factor 1 receptor inhibitor PLX3397 in recurrent glioblastoma: an Ivy Foundation Early Phase Clinical Trials Consortium phase II study. *Neuro Oncol.* 2016;18(4):557-64.
66. Audic Y, and Hartley RS. Post-transcriptional regulation in cancer. *Biology of the cell / under the auspices of the European Cell Biology Organization.* 2004;96(7):479-98.
67. Ben-Aharon I, Vidal L, Rizel S, Yerushalmi R, Shpilberg O, Sulkes A, et al. Bisphosphonates in the adjuvant setting of breast cancer therapy--effect on survival: a systematic review and meta-analysis. *PloS one.* 2013;8(8):e70044.
68. Gnant M, Mlineritsch B, Schippinger W, Luschin-Ebengreuth G, Postlberger S, Menzel C, et al. Endocrine therapy plus zoledronic acid in premenopausal breast cancer. *The New England journal of medicine.* 2009;360(7):679-91.
69. Sandhu SK, Papadopoulos K, Fong PC, Patnaik A, Messiou C, Olmos D, et al. A first-in-human, first-in-class, phase I study of carlumab (CNTO 888), a human monoclonal antibody against CC-

chemokine ligand 2 in patients with solid tumors. *Cancer Chemother Pharmacol.* 2013;71(4):1041-50.
70. Pienta KJ, Machiels JP, Schrijvers D, Alekseev B, Shkolnik M, Crabb SJ, et al. Phase 2 study of carlumab (CNTO 888), a human monoclonal antibody against CC-chemokine ligand 2 (CCL2), in metastatic castration-resistant prostate cancer. *Invest New Drugs.* 2013;31(3):760-8.
71. Nywening TM, Wang-Gillam A, Sanford DE, Belt BA, Panni RZ, Cusworth BM, et al. Targeting tumour-associated macrophages with CCR2 inhibition in combination with FOLFIRINOX in patients with borderline resectable and locally advanced pancreatic cancer: a single-centre, open-label, dose-finding, non-randomised, phase 1b trial. *The Lancet Oncology.* 2016;17(5):651-62.
72. Kobold S, Wiedemann G, Rothenfusser S, and Endres S. Modes of action of TLR7 agonists in cancer therapy. *Immunotherapy.* 2014;6(10):1085-95.
73. Chao MP, Alizadeh AA, Tang C, Myklebust JH, Varghese B, Gill S, et al. Anti-CD47 antibody synergizes with rituximab to promote phagocytosis and eradicate non-Hodgkin lymphoma. *Cell.* 2010;142(5):699-713.
74. Liu J, Wang L, Zhao F, Tseng S, Narayanan C, Shura L, et al. Pre-Clinical Development of a Humanized Anti-CD47 Antibody with Anti-Cancer Therapeutic Potential. *PloS one.* 2015;10(9):e0137345.
75. Racioppi L, Nelson ER, Huang W, Mukherjee D, Lawrence SA, Lento W, et al. CaMKK2 in myeloid cells is a key regulator of the immune-suppressive microenvironment in breast cancer. *Nature communications.* 2019;10(1):2450.
76. Svensson S, Abrahamsson A, Rodriguez GV, Olsson AK, Jensen L, Cao Y, et al. CCL2 and CCL5 Are Novel Therapeutic Targets for Estrogen-Dependent Breast Cancer. *Clinical cancer research : an official journal of the American Association for Cancer Research.* 2015;21(16):3794-805.
77. Ciucci A, Zannoni GF, Buttarelli M, Lisi L, Travaglia D, Martinelli E, et al. Multiple direct and indirect mechanisms drive estrogen-induced tumor growth in high grade serous ovarian cancers. *Oncotarget.* 2016;7(7):8155-71.
78. Ning C, Xie B, Zhang L, Li C, Shan W, Yang B, et al. Infiltrating Macrophages Induce ERalpha Expression through an IL17A-mediated Epigenetic Mechanism to Sensitize Endometrial Cancer Cells to Estrogen. *Cancer research.* 2016;76(6):1354-66.
79. Okamoto M, Udagawa N, Uehara S, Maeda K, Yamashita T, Nakamichi Y, et al. Noncanonical Wnt5a enhances Wnt/beta-catenin signaling during osteoblastogenesis. *Scientific reports.* 2014;4:4493.
80. Zhao F, Xiao C, Evans KS, Theivanthiran T, DeVito N, Holtzhausen A, et al. Paracrine Wnt5a-beta-Catenin Signaling Triggers a Metabolic Program that Drives Dendritic Cell Tolerization. *Immunity.* 2018;48(1):147-60 e7.
81. Haines CN, Wardell SE, and McDonnell DP. Current and emerging estrogen receptor-targeted therapies for the treatment of breast cancer. *Essays Biochem.* 2021.
82. Cocconi G, Bella M, Calabresi F, Tonato M, Canaletti R, Boni C, et al. Treatment of metastatic malignant melanoma with dacarbazine plus tamoxifen. *The New England journal of medicine.* 1992;327(8):516-23.
83. Lens MB, Reiman T, and Husain AF. Use of tamoxifen in the treatment of malignant melanoma. *Cancer.* 2003;98(7):1355-61.
84. Wardell SE, Marks JR, and McDonnell DP. The turnover of estrogen receptor alpha by the selective estrogen receptor degrader (SERD) fulvestrant is a saturable process that is not required for antagonist efficacy. *Biochem Pharmacol.* 2011;82(2):122-30.

85. McDonnell DP, Wardell SE, Chang CY, and Norris JD. Next-Generation Endocrine Therapies for Breast Cancer. *Journal of clinical oncology : official journal of the American Society of Clinical Oncology.* 2021;39(12):1383-8.
86. Martinkovich S, Shah D, Planey SL, and Arnott JA. Selective estrogen receptor modulators: tissue specificity and clinical utility. *Clinical interventions in aging.* 2014;9:1437-52.
87. Neubert NJ, Schmittnaegel M, Bordry N, Nassiri S, Wald N, Martignier C, et al. T cell-induced CSF1 promotes melanoma resistance to PD1 blockade. *Sci Transl Med.* 2018;10(436).
88. Bai X, Lin X, Zheng K, Chen X, Wu X, Huang Y, et al. Mapping endocrine toxicity spectrum of immune checkpoint inhibitors: a disproportionality analysis using the WHO adverse drug reaction database, VigiBase. *Endocrine.* 2020;69(3):670-81.
89. Ozdemir BC. Immune checkpoint inhibitor-related hypogonadism and infertility: a neglected issue in immuno-oncology. *J Immunother Cancer.* 2021;9(2).
90. Ohata C, Tadokoro T, and Itami S. Expression of estrogen receptor beta in normal skin, melanocytic nevi and malignant melanomas. *J Dermatol.* 2008;35(4):215-21.
91. Clausen BE, Burkhardt C, Reith W, Renkawitz R, and Forster I. Conditional gene targeting in macrophages and granulocytes using LysMcre mice. *Transgenic Res.* 1999;8(4):265-77.
92. Overwijk WW, Theoret MR, Finkelstein SE, Surman DR, de Jong LA, Vyth-Dreese FA, et al. Tumor regression and autoimmunity after reversal of a functionally tolerant state of self-reactive CD8+ T cells. *The Journal of experimental medicine.* 2003;198(4):569-80.
93. Nelson ER, Wardell SE, Jasper JS, Park S, Suchindran S, Howe MK, et al. 27-Hydroxycholesterol links hypercholesterolemia and breast cancer pathophysiology. *Science.* 2013;342(6162):1094-8.

Figure 1

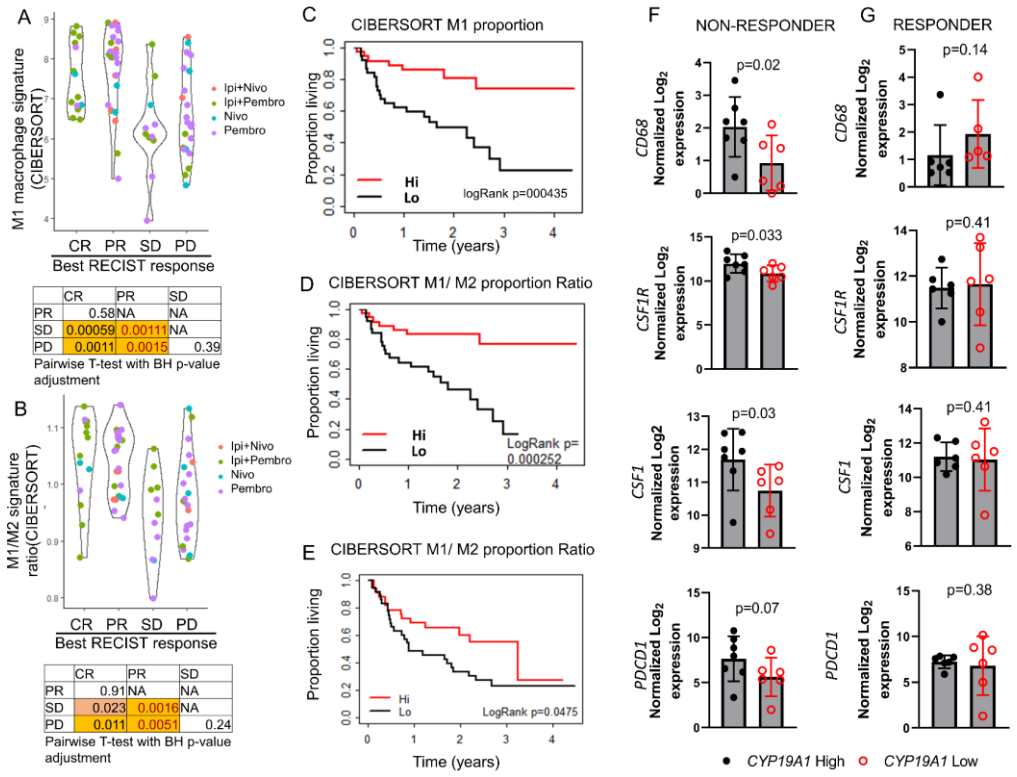

Figure 1. Decreased M1/M2 ratio compromises benefit to immunotherapy in melanoma patients. (A-B) Relative proportion of M1 macrophages as determined by CIBERSORT or the ratio of M1/M2 macrophages in melanoma patients parsed by their response to immunotherapies in same patient cohort. **(C-D)** Median overall survival in all patient cohorts (Gide *et al.*) treated with immunotherapy with either high or low proportions of M1 macrophages or M1/M2 ratio as determined by CIBERSORT. **(E)** Median overall survival in all patient cohorts treated with Ipilimumab alone (Van Allen *et al*) or either Pembrolizumab or Nivolumab alone (Hugo *et al*), with either high or low M1/M2 signature ratio as determined by CIBERSORT. **(F-G)** *CD68, CSF1, CSF1R* and *PDCD1* expression in melanoma patients who were classified as non-responders (n=13) and responders (n=12) to anti-PD1 therapy, obtained from the Hugo *et al* datasets. Both responders and non-responders were stratified to *CYP19A1*^{hi} and *CYP19A1*^{lo} by median expression. Significance was calculated using a paired t test (A, C, D and E), unpaired t test (J and K) and by log rank test (B, F, G, H and I).

Figure 2

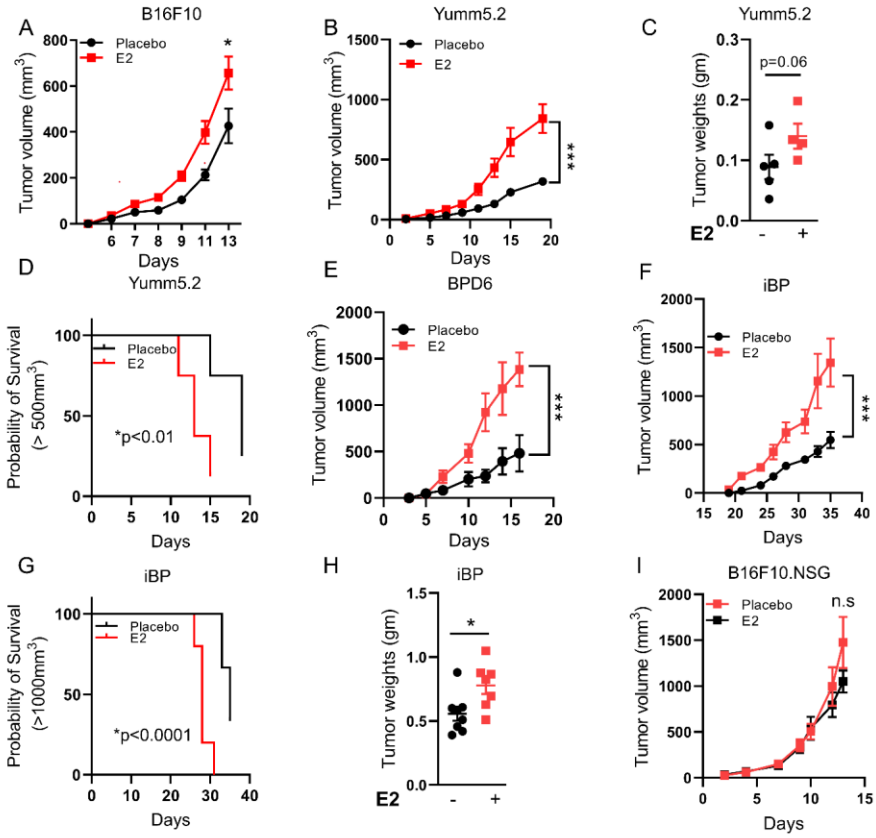

Figure 2. E2 promotes melanoma tumor growth. (A-B, E) Subcutaneous tumor growth of B16F10 ($1X10^5$ cells) n=10 or Yumm5.2 ($0.5x10^5$ cells) n=8, or BPD6 ($0.5x10^5$ cells) n=5 cells in syngeneic C57BL/6J ovariectomized hosts supplemented with placebo or E2. **(C)** Weights of YuMM5.2 tumors, resulting from experiments in 1B. (**D**) Survival of mice harboring YuMM5.2 tumors resulting from experiment 1B **(F)** Tumor growth in iBP female mice that were ovariectomized and supplemented with either placebo or E2 pellets (n=5). Tumor formation in these mice were induced with a single intradermal dose of 150µg of 4-hydroxytamoxifen (4OHT). **(G-H)** Survival and weights of tumors (Placebo vs E2), n=6, resulting from experiments in 1F. **(I)** B16F10 ($1X10^5$ cells) n=10, tumor growth in ovariectomized NSG (NOD.Cg-*Prkdc*^{scid} *Il2rg*^{tm1Wjl}/SzJ) mice supplemented with placebo or E2. A, B, E and F representative of two independent experiments. Data are expressed as mean ± S.E.M. Significance was calculated using the Student's t test (C and H), log-rank test (D and G) and two-way ANOVA followed by Bonferroni's multiple correction (A, B, E, F and I) *p<0.05, **p<0.01 and ***p<0.001

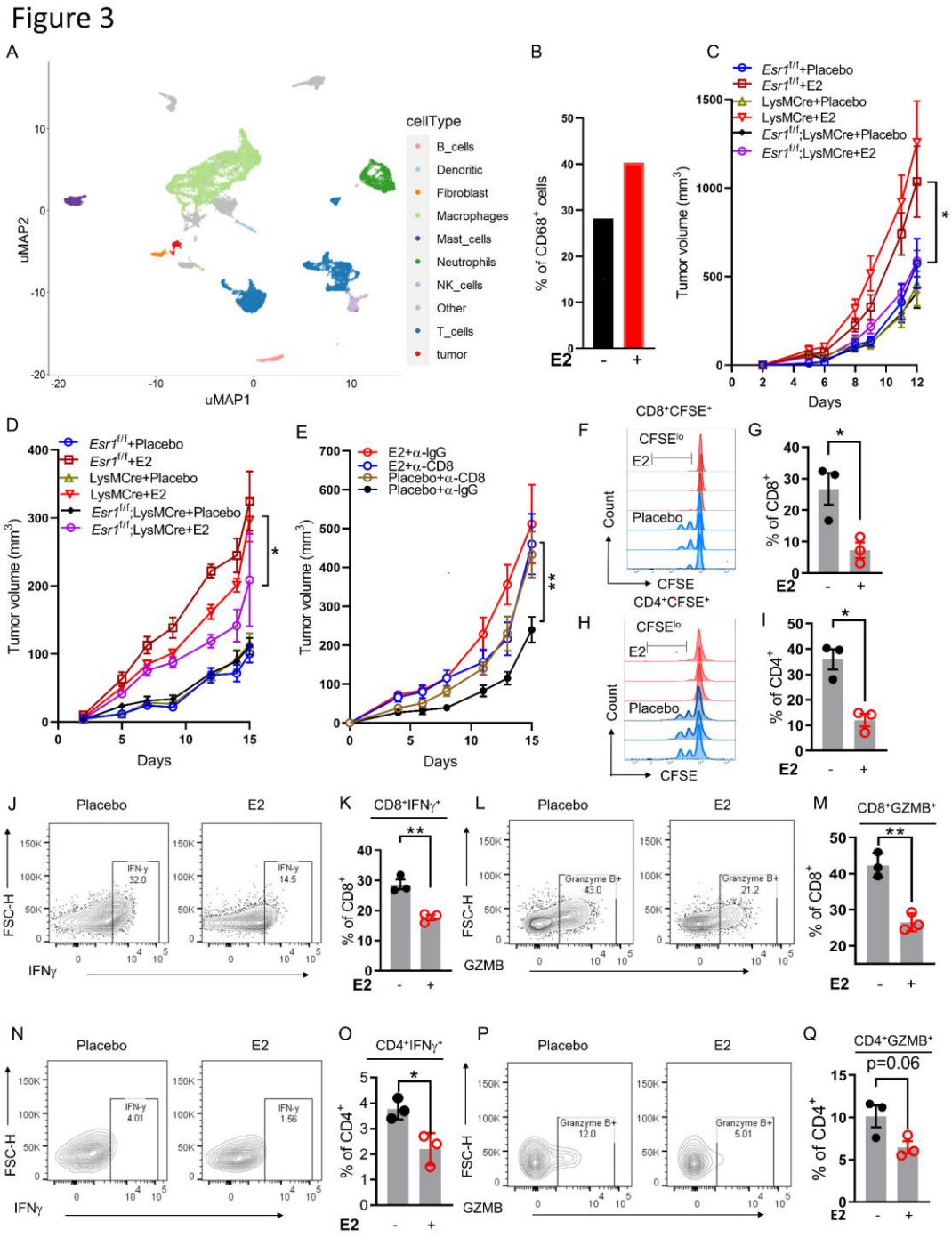

Figure 3. E2 regulates myeloid cell function in the tumor microenvironment. (A-B) Uniform manifold approximation and projection (uMAP) plots of expression profiles for tumor infiltrating immune cells (CD45$^+$) (n=3 tumors/treatment, pooled together) isolated from iBP tumors. Each dot represents an individual cell **(A)**. Percentage of CD68$^+$ macrophages/monocytes among all sequenced cell types determined by scRNA seq in placebo vs E2 treated samples **(B)**. **(C-D)** Syngeneic tumor growth of B16F10 (1x10^5) cells and YuMM5.2 (5x10^5) cells in myeloid ERα knockout (*Esr1*$^{f/f}$;LysMCre) and littermate control (*Esr1*$^{f/f}$ and LysMCre) mice were ovariectomized and supplemented with either placebo or E2 pellets. *Esr1*$^{f/f}$+ Placebo, (blue, n= 10); LysMCre+Placebo, (brown, n= 7); *Esr1*$^{f/f}$;LysMCre+Placebo, (black, n= 8); *Esr1*$^{f/f}$+E2, (maroon, n= 8); LysMCre+E2, (red, n= 7); *Esr1*$^{f/f}$;LysMCre+E2, (purple, n= 8). **(E)** Tumor growth of YuMM5.2 ((5x10^5) in CD8+T cell depleted C57BL6/J hosts that were ovariectomized and supplemented with placebo and E2 (n= 8 mice per treatment). **(F- I)** T cell proliferation was assessed after co-culturing with tumor infiltrating CD11b$^+$ cells isolated from iBP mice treated with either placebo or E2. Representative CFSE dilution plots of CD8$^+$ (F) and CD4$^+$**(H)** cells. Quantification of CFSE low/negative CD8$^+$ **(G)** and CD4$^+$ **(I)** populations and expressed as percentage of CD8$^+$ and CD4$^+$ T cells (n=3), representative of two independent experiments. **(J-Q)** Representative flow cytometry plots and percentage of IFNγ$^+$ and GZMB$^+$ CD8$^+$ T **(J-M)** or CD4$^+$ T cells **(N-Q)** after 72 hours of co-culture with tumor infiltrating CD11b+ myeloid cells isolated from iBP mice treated with either placebo or E2, n=3 per group. Data are represented as mean ±S.E.M. Significance was calculated using a Student's t test (G, I, K, M, O and Q) and by two-way ANOVA (C, D and E) followed by Bonferroni's multiple correction. *p<0.05, **p<0.01 and ***p<0.001.

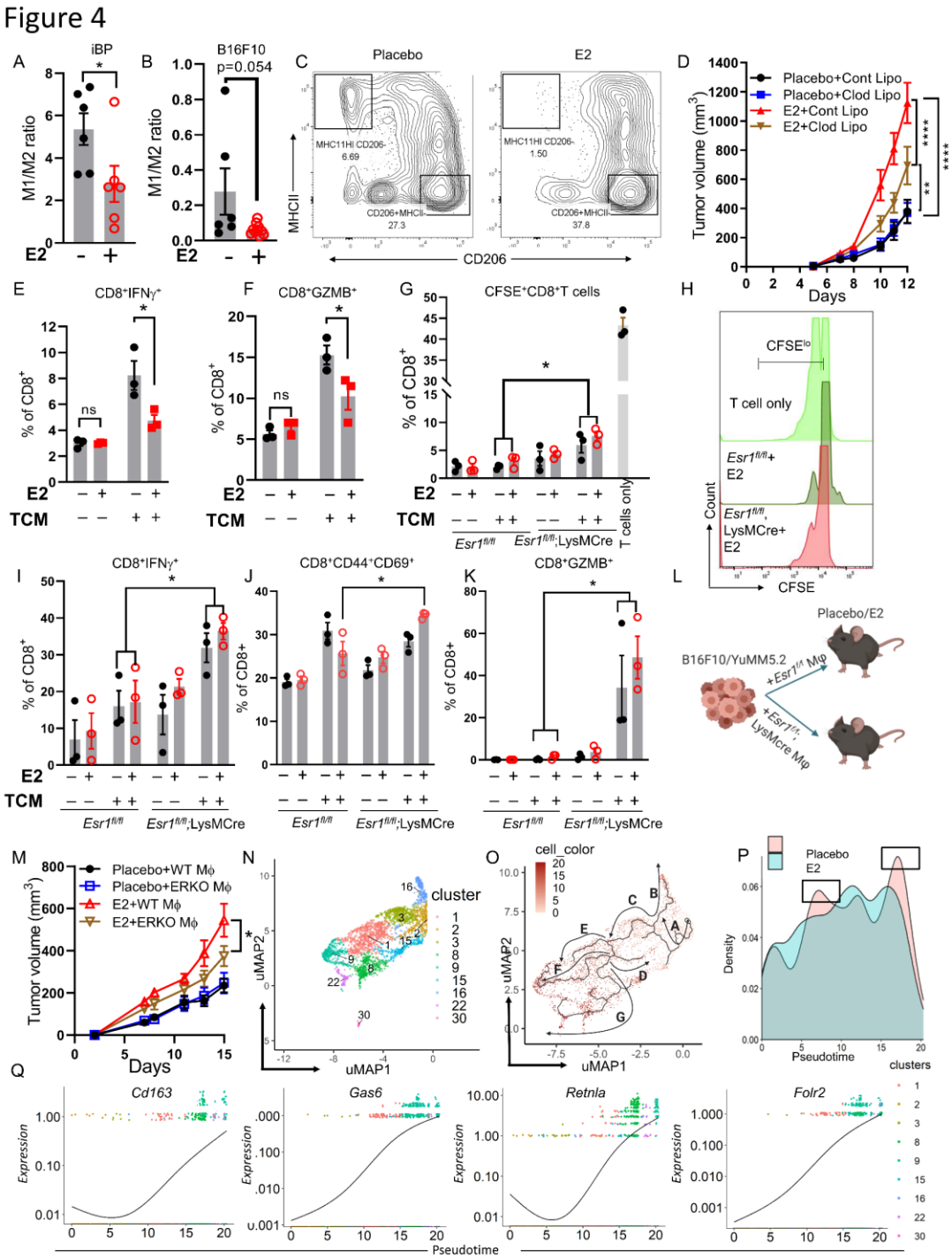

Figure 4. E2 regulates TAM function. (A-C) Ratio of M1 to M2 macrophages in iBP (n=6) **(A)** and B16F10 (n=6-10) tumors **(B)** from placebo and E2 treated mice and representative flow cytometry plots of M2 and M1 macrophages in the B16F10 model **(C)**. **(D)** Growth of B16F10 tumors (n=12) upon depletion of macrophages by clodronate liposomes in ovariectomized mice supplemented with placebo or E2. **(E-F)** Quantification of IFNγ$^+$CD8$^+$ T (E) and GZMB$^+$CD8$^+$ T **(F)** cells (n=3) that were cocultured with BMDM differentiated in NM or TCM and treated with either DMSO or E2 (1nM). **(G-H)** CFSE dilution and quantification representing proliferation of CFSE$^{low/-}$ CD8$^+$ T (n=3) after co-culturing with BMDM cells from *Esr1*$^{f/f}$ and *Esr1*$^{f/f}$;LysMCre mouse, differentiated in either normal media or TCM (B16F10), followed by treatment with either DMSO or E2 (1nM). **(I-K)** Quantification of IFNγ$^+$, CD44$^+$CD69$^+$ and GZMB+ CD8 T cells (n=3) from the same experiment as in G. **(L)** Tumor co-mixing methodology. **(M)** Syngeneic tumor growth of YuMM5.2 (5X10^5) cells co-mixed with BMDM from either (*Esr1*$^{f/f}$;LysMCre) or its littermate controls (*Esr1*$^{f/f}$) (1:1) in ovariectomized mice supplemented with either placebo or E2. (*Esr1*$^{f/f}$ BMDM+YuMM5.2) - placebo (black, n= 10), (*Esr1*$^{f/f}$;LysMCre, BMDM+YuMM5.2)-placebo (blue, n= 10), (*Esr1*$^{f/f}$ BMDM+YuMM5.2)- E2 (red, n= 10) and (*Esr1*$^{f/f}$;LysMCre, BMDM+YuMM5.2)-E2 (brown, n= 10). **(N)** UMAP representation of macrophage/monocyte subclusters as determined from scRNA sequencing. **(O)** Trajectory analysis depicting the differentiation of monocytes into different lineages of macrophages. **(P)** Density of cells in macrophage/monocyte subclusters along a pseudotime gradient. **(Q)** Expression of M2 associated genes (*Cd163*, *Lgr2, Retnla and Folr2*) in macrophage clusters along the pseudotime axis. E-F and G-K, representative of two independent experiments. Data are expressed as individual data points and represented by mean ±S.E.M. Significance was calculated by Student's t test (A-B), one-way ANOVA (E-G, I-K) and by two-way ANOVA (D and M) followed by Bonferroni's multiple correction (*p<0.05, **p<0.01 and ***p<0.001).

Figure 5

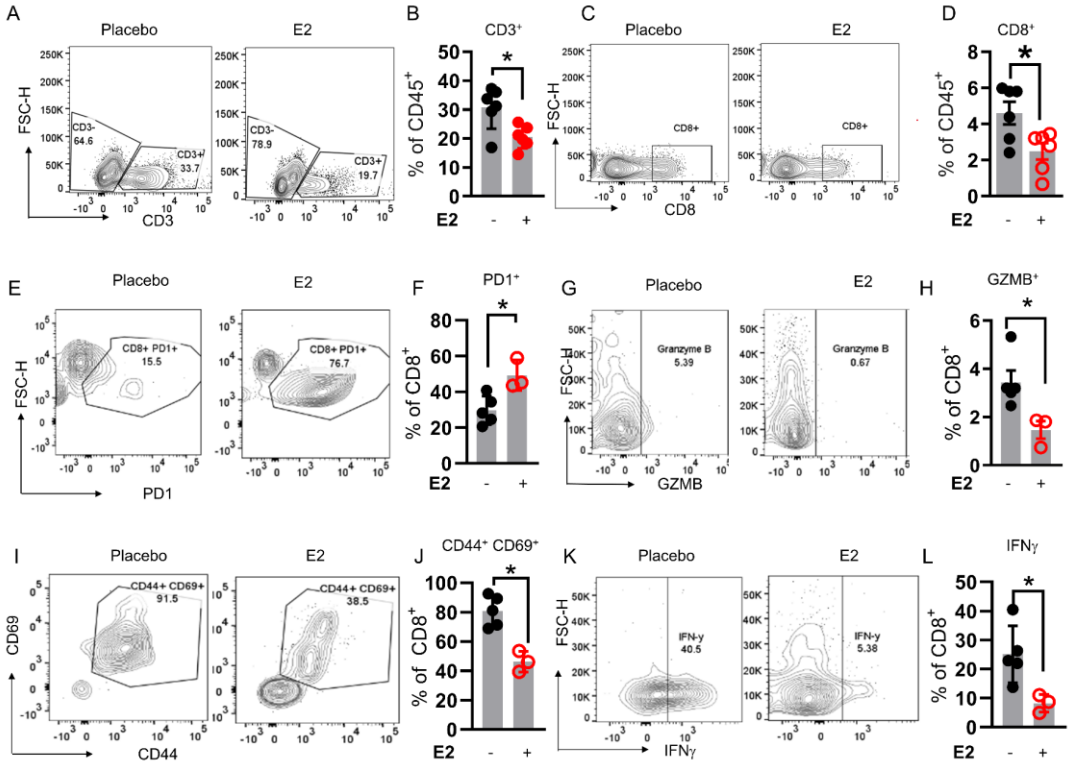

Figure 5. E2 suppresses anti-tumor T cell response. Representative flow cytometry plots and quantification of CD3+ **(A-B)** and CD8+ **(C-D)** tumor infiltrating lymphocytes in iBP (n=5-6) tumors isolated from mice treated with either placebo (black) or E2 (red). **(E-L)** Representative flow cytometry plots and quantification of PD1+ **(E-F)**, GZMB+**(G-H)**, CD44+CD69+ **(I-J)** and IFNγ+ **(K- L)** CD8+ T cells in YuMM5.2 tumors from mice treated with placebo (black) or E2 (red) (n=3-5) **(H)**. Data are expressed as individual data points and are represented as mean ± S.E.M. Significance was calculated using the Student's t test. (*p<0.05, **p<0.01 and ***p<0.001.)

Figure 6

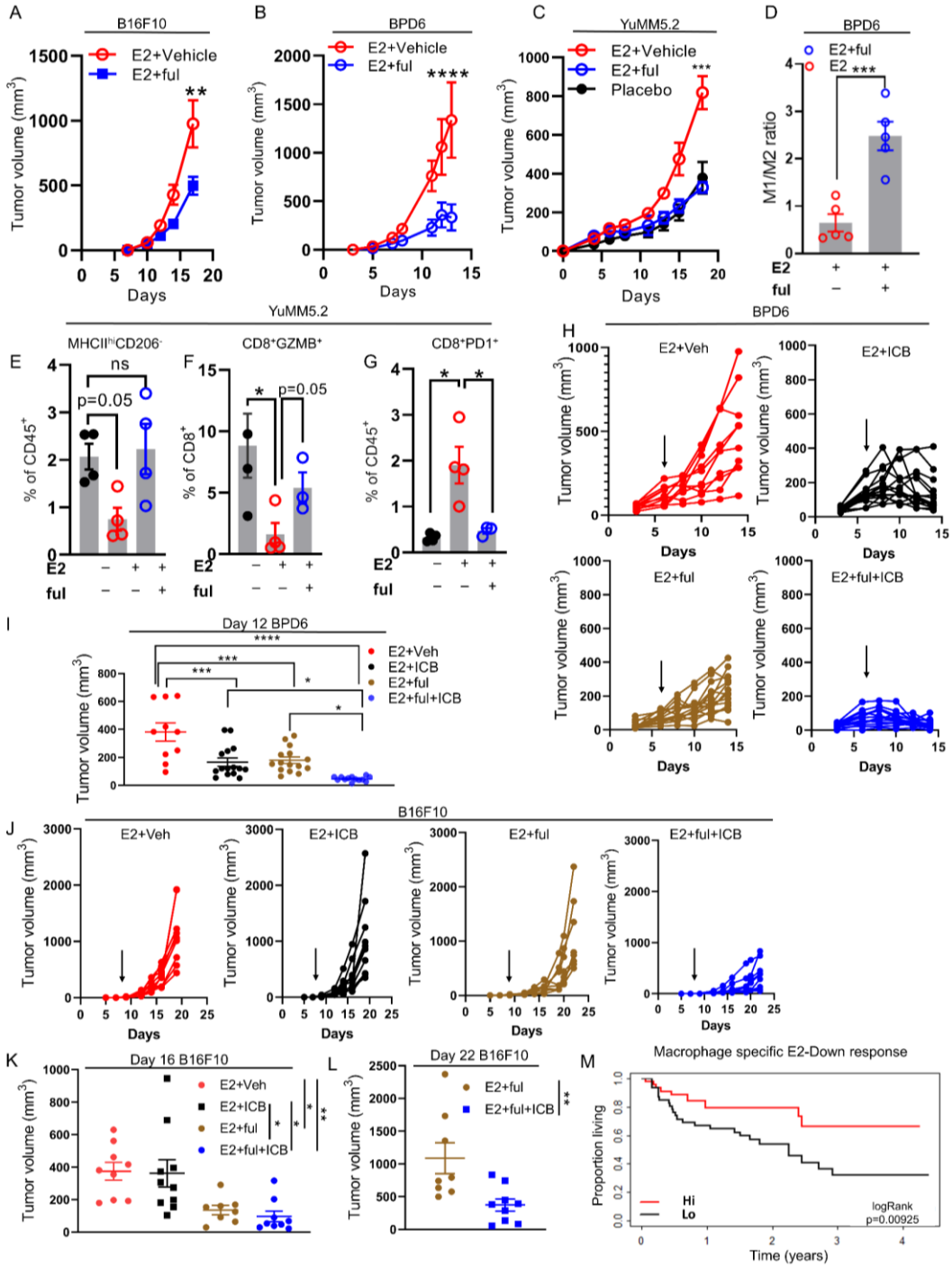

Figure 6. Pharmacological depletion of ER reverses E2 dependent melanoma tumor growth. (A-C) Growth of B16F10 ($0.5X10^5$) (n=9), YuMM5.2 ($5x10^5$) (n=6) and BPD6 ($5x10^5$) (n=5) tumors in ovariectomized C57BL/6J mice supplemented with placebo or E2 and co-treated with the ERα antagonist fulvestrant. **(D)** Quantification of the ratio of M1 and M2 macrophages isolated from BPD6 tumors (B) **(E-G)** Quantification of M1 macrophages ($MHCII^{hi}$ $CD206^{-ive}$), $GZMB^+CD8^+$ T cells and $PD1^+CD8^+$ T cells in YuMM5.2 tumors from 6C (n=4). **(H)** Individual volumes of BPD6 tumors implanted in ovariectomized mice treated with placebo or E2 following co-treatment with fulvestrant and ICB (anti PD1+anti CtLA4) either alone or in combination. Vehicle+IgG (n=10, red), fulvestrant+IgG (n=15, blue), vehicle+ICB (n=15, black) and fulvestrant+ ICB (n=15 brown). Black arrow indicates start of ICB treatment regimen. **(I)** Tumor volumes of BPD6 measured at day 12 after inoculation. **(J)** Individual tumor volumes of B16F10 ($0.5x10^5$) implanted in ovariectomized C57BL6/J mice supplemented with placebo and E2 and co-treated with fulvestrant along with ICB (anti-PD1). Vehicle+IgG (n=9, red), fulvestrant+IgG (n=8, blue), vehicle+ICB (n=9, black) and fulvestrant+ ICB (n=10 brown). Black arrow indicates start of anti-PD1 treatment regimen. **(K-L)** Tumor volumes of B16F10 measured at day 16 (all 4 groups) and day 22 (E2+ful vs E2+ful+anti-PD1) group after inoculation. **(M)** Median overall survival in all patients treated with immunotherapy (Pembrolizumab or Nivolumab alone, or in combination with Ipilimumab) from the Gide *et. al* dataset with either high or low E2-down-regulated gene signatures derived from CD68+ cells in the scRNA seq. A, B and C representative of two individual experiments. Data are expressed as mean ±S.E.M. Significance was calculated by one-way ANOVA followed by Bonferroni's multiple correction (K) by Student's t test (L) and by log rank test (M). *p<0.05, **p<0.01 and ***p<0.001.